Novel dynamical mode in a tilted smectic liquid-crystal film

M. S. Spector, S. Sprunt, and J. D. Litster
Department of Physics, Massachusetts Institute of Technology, Cambridge, Massachusetts 02139-4307
(Received 6 October 1992)

We report on light-scattering experiments in the smectic-*C* phase of a two-dimensional, freely suspended liquid-crystal film at wave vectors intermediate between pure bend and splay director fluctuations. The dynamic signal reveals the presence of two diffusive modes, one of which is the usual hydrodynamic mode for in-plane director fluctuations and one of which has not been previously reported. The wave-vector dependence of the scattered intensity for the new mode is well described by the selection rules for out-of-plane fluctuations (undulations) of the film. However, the overdamped dynamics reveal a nonhydrodynamic and extremely slow decay, in contrast to the usual picture for smectic layer undulations. Near the smectic-*C* to smectic-*I* (hexatic) transition, the elastic moduli and decay constants associated with the two modes show a remarkably similar temperature dependence.

PACS number(s): 61.30.Eb, 64.70.Md, 78.35.+c

In smectic-*C* (Sm-*C*) liquid crystals, it is well known that fluctuations of the molecular orientations in the smectic planes give rise to strong nematiclike Rayleigh scattering. Early light-scattering studies on bulk samples confirmed this behavior [1], which was first proposed by the Orsay group [2]. More recent experiments on free-standing films have studied the so-called bend and splay geometries in the Sm-*C* phase, in which the scattering wave vector **q** is either in or normal to the plane containing the director and the layer normal [3–5]. In both these geometries, a single hydrodynamic mode is found that corresponds to fluctuations in the orientation of the in-plane director component **n**. In this paper, we describe experiments in which the orientation of the scattering wave vector is varied between these two geometries at fixed magnitude (χ scans). These scans reveal a previously unreported diffusive mode in addition to the fluctuations of **n**. The χ dependence of the intensity from this mode leads us to associate it with undulations of the film. Our results indicate that it is coupled to the in-plane fluctuations. We also show scans where the magnitude of **q** is varied at fixed orientation (q scans) and discuss the temperature dependence of the in-plane elastic constants and the layer bending elasticity.

The liquid crystal studied in this experiment is racemic 4-(2-methylbutyl)-phenyl-4′-(octyloxy)-(1,1′)-biphenyl-4-carboxylate (abbreviated 8OSI), which has the bulk phase sequence isotropic→nematic→Sm-*A*→Sm-*C*→Sm-*I*→Sm-*J*. This material has been extensively studied at the Massachusetts Institute of Technology using x-ray scattering [6], light scattering [7], and heat-capacity measurements [8]. Details of the Sm-*C* to Sm-*I* transition, and other properties of the Sm-*I* phase, may be found in these references.

In our experimental setup, the sample is illuminated by an argon-ion laser ($\lambda=5145$ Å) with polarization normal to the scattering plane. We observe the depolarized component of the scattered light at a scattering angle θ imaged onto a photomultiplier tube. The film is maintained in an atmosphere of 100 Torr of dry nitrogen gas. Temperature stability is ~5 mK during the χ scans. Further details of our film oven are available elsewhere [7]. Our scattering geometry is shown schematically in Fig. 1. We will consider this problem in the coordinate system of the film, where the equilibrium position of the director is in the xz plane, with **z** being defined along the equilibrium layer normal. In this reference frame, the film remains fixed and the scattering plane is rotated by an angle χ from the xz plane. The incident wave vector and polarization are given by $\mathbf{k}_i = nk_0\mathbf{z}$ and $\boldsymbol{\pi}_i = -\mathbf{x}\sin\chi + \mathbf{y}\cos\chi$, and the scattered wave vector and polarization are given by $\mathbf{k}_f = nk_0(\mathbf{x}\sin\theta\cos\chi + \mathbf{y}\sin\theta\sin\chi + \mathbf{z}\cos\theta)$ and $\boldsymbol{\pi}_f = \mathbf{x}\cos\theta\cos\chi + \mathbf{y}\cos\theta\sin\chi - \mathbf{z}\sin\theta$ where $k_0 = 2\pi/\lambda$

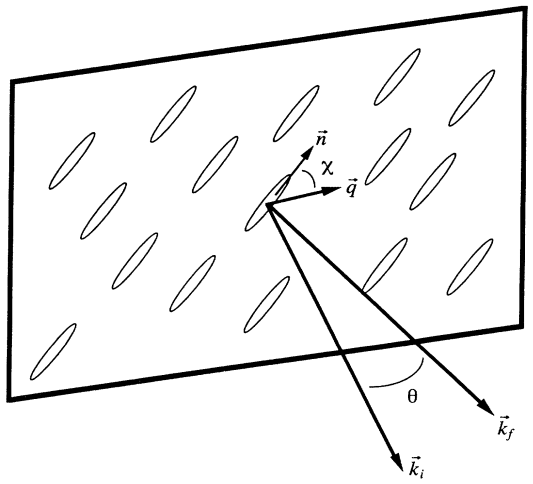

FIG. 1. Experimental geometry used in the light-scattering experiments. The incident wave vector $\mathbf{k}_i$ is normal to the smectic (and film) plane, and light with scattered wave vector $\mathbf{k}_f$ is detected. The in-plane component of the director **n** forms an equilibrium angle of χ with the plane containing the incident and scattered wave vectors.

and n is the refractive index of the film.

We begin by describing χ scans in which the oven is rotated between the bend geometry ($\chi=0°$) and the splay geometry ($\chi=90°$) at fixed θ. In general, the intensity autocorrelation function is made up of two components. The first mode has a decay time typical of light-scattering experiments (~ 10 kHz), which we associate with the usual fluctuations of **n**; the second mode is a much slower mode (~ 1 Hz). Figure 2 displays intensity autocorrelation measurements at four values of χ in a four-layer film. At each point, two correlation functions are taken consecutively on our 64-channel correlator. For the first correlation function, a sample time of $\sim 1-10$ μsec is used, while for the second we always use a sample time of 10 msec. The results are combined in a double-exponential fit, which are the lines shown in Fig. 2. The inset shows the long-time scale results expanded with the $\chi=0°$ data scaled down onto the same plot. No second decay is observed at $\chi=0°$ and at $\chi=90°$, where the long-time correlation function is constant. Another important feature we observe is that the decay time for the fast mode (τ_f) is substantially different at $\chi=30°$ and at $\chi=60°$, while that for the slow mode (τ_s) is approximately the same. In Figs. 3 and 4, we show the χ dependence of the intensities and linewidths, respectively. The relatively poor determination of $\Gamma_s=1/\tau_s$ comes from the fits to the slow correlation functions, as seen in the inset of Fig. 2. Attempts to fit the slow correlation functions using cumulants or terms to account for possible heterodyning did not produce better results. We also point out that it was necessary to run the laser at low power during these scans to avoid overflowing the four-bit correlator at long sample times. The fits used in these scans will be discussed further below.

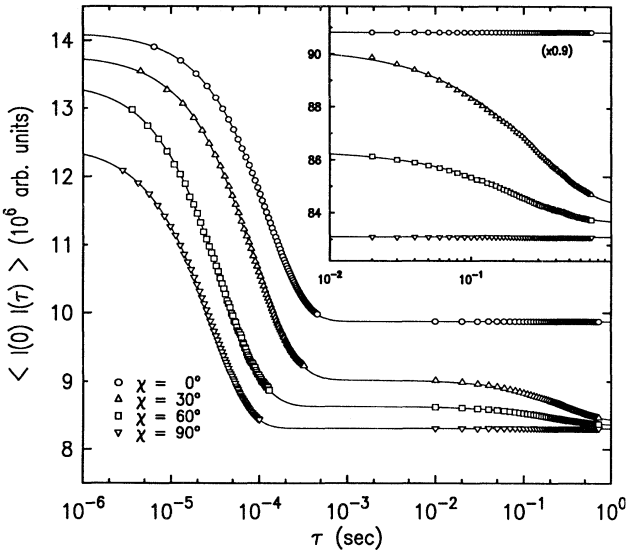

FIG. 2. Autocorrelation functions at $\chi=0°$, 30°, 60°, and 90° for a four-layer 8OSI film in the Sm-C phase at $T=102$ °C. Inset: long-time scale results expanded with the results at $\chi=0°$ scaled down by 0.9. The solid line is a double-exponential fit. The intensities have been arbitrarily adjusted for convenience of display.

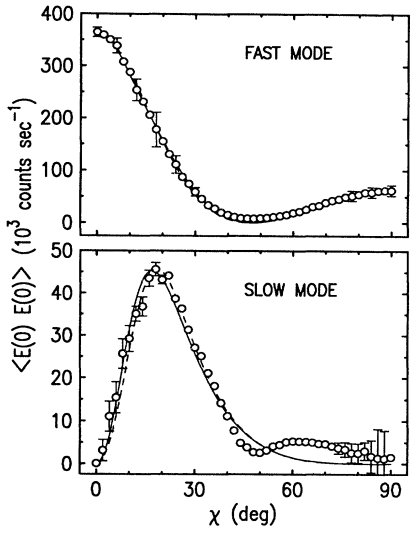

FIG. 3. Intensity of scattering from the two modes as a function of scattering vector orientation χ at fixed scattering angle, $\theta=4°$, for a four-layer 8OSI film in the Sm-C phase at $T=102$ °C. The lines are a fit to the two components of Eq. (7). In the top panel, the intensity of the fast mode is shown fit to g_1^2/λ_1, while the slow-mode fit to g_2^2/λ_2 is shown in the bottom panel. The two intensities are fit to the same parameters. The solid lines allow for a nonzero coupling, while the dashed lines fix $D_1=D_2=0$; all fits have $\sigma=0$. For clarity, the error bars are only shown for every third point in the top panel.

In order to obtain more detailed information about this new slow mode, we performed a series of scans where we varied the magnitude of **q** at fixed orientation. The results of these scans for $\chi=30°$ are shown in Figs. 5 and 6.

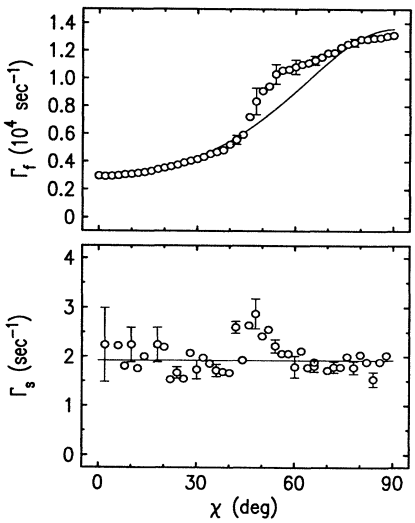

FIG. 4. Linewidth of the two modes as a function of scattering orientation χ at fixed scattering angle, $\theta=4°$, for a four-layer 8OSI film in the Sm-C phase at $T=102$ °C. In the top panel, Γ_f of the fast mode is shown fit to $\lambda_1(\mathbf{q})/\eta$ using the values of λ_1 derived from the fits in Figs. 3 and 5. In the bottom panel, Γ_s of the slow mode is shown fit to a constant value of 1.92 sec^{-1}.

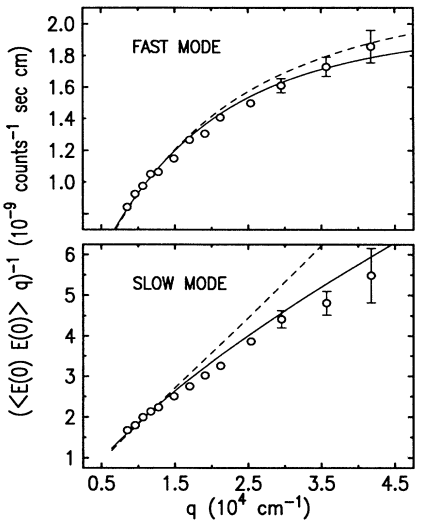

FIG. 5. Reciprocal of the intensity multiplied by q for the two modes is plotted as a function of the magnitude of the in-plane scattering vector q. This is for a four-layer 8OSI film in the Sm-C phase at $T=102\,^{\circ}$C with fixed orientation $\chi=30^{\circ}$. Fits are to the same parameters as in Fig. 3. The solid lines allow for a nonzero coupling, while the dashed lines fix $D_1=D_2=0$; both fits have $\sigma=0$.

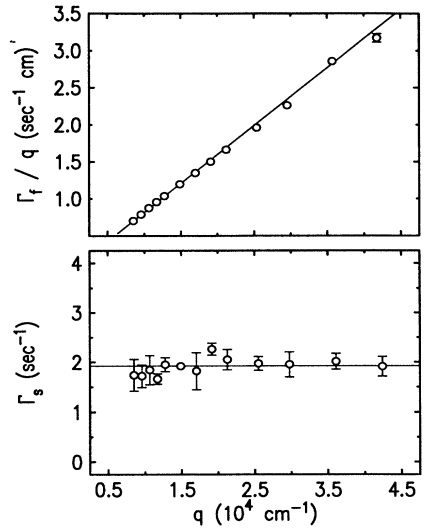

FIG. 6. Linewidth dispersion of the two modes at fixed orientation, $\chi=30^{\circ}$, for a four-layer 8OSI film in the Sm-C phase at $T=102\,^{\circ}$C. In the top panel, Γ_f of the fast mode is shown fit to q^2. In the bottom panel, Γ_s of the slow mode is shown fit to the same constant value of 1.92 sec^{-1} as in Fig. 4.

In Fig. 5, we show $(Iq_\perp)^{-1}$ plotted against $q_\perp$, where $I=\langle E(0)E(0)\rangle$ is the intensity of the fast or slow mode. Downward curvature of the data indicates that the intensity decays more slowly than q^{-2}. The significance of this will be discussed below. In Fig. 6, we show the linewidth of the two modes versus q. As expected, the linewidth of the fast mode has a hydrodynamic behavior, $\Gamma_f \sim q^2$. However, the slow-mode decay time seems to be independent of $\mathbf{q}$, both in magnitude (Fig. 6) and orientation (Fig. 4). Both sets of data indicate a constant value for Γ_s of about 1.9 sec^{-1} at $T=102\,^{\circ}$C. This result is quite surprising, and we know of no hydrodynamic theory that accounts for this behavior. However, we may explain most of the features of the static behavior (intensity) using a model free energy that includes distortion of the film surface.

We consider a bulk free-energy density for the Sm-C phase that includes fluctuations in the phase ϕ of the tilt order parameter $\Phi\equiv\Phi_0 e^{i\phi}$ and undulations of the film described by transverse displacements of the layers by u. Here Φ_0 is the angle the director makes with the layer normal, and ϕ is the angle between the in-plane director component and the $\mathbf{x}$ axis. The free energy per unit volume can be written as [2,9]

$$
\begin{aligned}
F_d(\mathbf{r}) = \frac{1}{2}\left[B_1\left(\frac{\partial\phi}{\partial x}\right)^2 + B_2\left(\frac{\partial\phi}{\partial y}\right)^2 + B_3\left(\frac{\partial\phi}{\partial z}\right)^2 + 2B_{13}\left(\frac{\partial\phi}{\partial z}\,\frac{\partial\phi}{\partial x}\right)\right] \\
+ \frac{1}{2}\left[C_1\left(\frac{\partial^2 u}{\partial x^2}\right)^2 + 2C_{12}\left(\frac{\partial^2 u}{\partial x^2}\,\frac{\partial^2 u}{\partial y^2}\right) + C_2\left(\frac{\partial^2 u}{\partial y^2}\right)^2\right] + \tfrac{1}{2}\bar{B}\left(\frac{\partial u}{\partial z}\right)^2 \\
+ \left[D_1\left(\frac{\partial^2 u}{\partial x\,\partial y}\,\frac{\partial\phi}{\partial x}\right) + D_2\left(\frac{\partial^2 u}{\partial y^2}\,\frac{\partial\phi}{\partial y}\right)\right] .
\end{aligned}
\tag{1}
$$

The first part of Eq. (1) is the usual elasticity associated with the distortions of the director field, which is analogous to a two-dimensional nematic phase [10]. The second term is the curvature elasticity of the layers plus a compressional term ($\bar{B}$), and the last part represents coupling between layer curvature and director-field distortions, which reflects how a deformation of the in-plane director affects the curvature of the smectic planes [9]. Since we consider only thin films, where $q_z \ll 2\pi/l$ (l is the film thickness), we may assume that the layers are incompressible and drop partial derivatives with respect to z. Therefore, in the following, $\mathbf{q}\equiv\mathbf{q}(x,y)$ represents the in-plane component of the momentum transfer. de Gennes [9] has suggested that when $q_z\neq 0$, the fluctuations of the layers are weak owing to the $\bar{B}$ term, but in a thin film where q_z is effectively zero, the fluctuations of the Sm-C director become strongly coupled to the undulation mode so we might expect the final term in (1) to be significant. Rewriting Eq. (1) in two-dimensional (2D) reciprocal space and integrating over z, we obtain the free

energy per unit area of the film:

$$F_{2D}(\mathbf{q})=\tfrac{1}{2}(K_B q_x^2+K_S q_y^2)|\phi(\mathbf{q})|^2 +\sigma(q_x^2+q_y^2)|u(\mathbf{q})|^2 +\tfrac{1}{2}l(C_1 q_x^4+2C_{12}q_x^2q_y^2+C_2 q_y^4)|u(\mathbf{q})|^2 +\tfrac{1}{2}l(D_1 q_x^2+D_2 q_y^2)[iq_y u(\mathbf{q})\phi^*(\mathbf{q})-iq_y u^*(\mathbf{q})\phi(\mathbf{q})], \tag{2}$$

where we replaced $B_1 l$ and $B_2 l$ by the more familiar 2D Frank elastic constants K_B and K_S, respectively; these represent the bendlike and splaylike distortions of the in-plane director field. As the film may be very thin, we have also added the second line in Eq. (2) to include the effects of the two free surfaces; σ is surface tension at *each* surface. In our analysis, we shall neglect this surface-tension term, and will justify this neglect below. Near the Sm-C to Sm-I transition, one should also include the fluctuations of the hexatic order parameter $\Psi_6\equiv\psi_6 e^{i\theta_6}$ [11]. Following Ref. [7], in which it was found that for *thin* films of 8OSI, θ_6 and ϕ are strongly coupled, we may take $\theta_6=\phi$. In that case, the important part of the free energy for light scattering is the same as in Eq. (2), with the in-plane elastic constants now defined in terms of two components,

$$K_B\equiv K_1^B+K_6^{\mathrm{I}},\quad K_S\equiv K_1^S+K_6^{\mathrm{II}}\ ,$$

where we use notation consistent with Ref. [7]. $K_1^{B,S}$ are the Sm-C in-plane director elastic constants and $K_6^{\mathrm{I,II}}$ are the bond elasticity constants for distortions with $\mathbf{q}$ along and normal to the tilt direction, respectively, for a two-dimensional system. Theoretically, one expects the hexatic (Sm-I) phase to be stable when $K>72k_B T_{CI}/\pi$ [12]. This result holds for an *isotropic* system. Previous results from 8OSI indicate that this condition does not separately apply to K_B and K_S [7].

In order to calculate the light scattering, we must diagonalize Eq. (2). Since u and ϕ have different dimensions, this requires a sensible choice of normal-mode coordinates. One possible choice would be ϕ and $\Omega\equiv-\partial u/\partial x=-iq_x u$, where Ω represents rotations of the director about the y axis or, equivalently, fluctuations of the tilt angle Φ_0. This choice, however, leads to terms in the free energy such as $\frac{1}{2}C_2(q_y^4/q_x^2)\Omega^2(\mathbf{q})$, which diverge in specific experimental geometries, e.g., $q_x=0$. A better alternative is to choose ϕ and $\psi\equiv-iq_0 u$, where $q_0=|\mathbf{q}|=k_0\sin\theta$. With this choice, Eq. (2) may be written

$$F_{2D}(\mathbf{q})=\tfrac{1}{2}\alpha(\mathbf{q})|\psi(\mathbf{q})|^2+\tfrac{1}{2}\beta(\mathbf{q})|\phi(\mathbf{q})|^2 -\tfrac{1}{2}\gamma(\mathbf{q})[\psi(\mathbf{q})\phi^*(\mathbf{q})+\psi^*(\mathbf{q})\phi(\mathbf{q})]\ , \tag{3}$$

where

$$\alpha(\mathbf{q})\equiv 2\sigma+(C_1 lq_x^4+2C_{12}lq_x^2q_y^2+C_2 lq_y^4)/q_0^2\ ,$$

$$\beta(\mathbf{q})\equiv K_B q_x^2+K_S q_y^2\ ,$$

$$\gamma(\mathbf{q})\equiv(D_1 lq_x^2+D_2 lq_y^2)q_y/q_0\ .$$

We define the normal modes $e_1(\mathbf{q})\equiv a\phi(\mathbf{q})+b\psi(\mathbf{q})$ and $e_2(\mathbf{q})\equiv b\phi(\mathbf{q})-a\psi(\mathbf{q})$, with $a^2+b^2=1$, such that

$$F_{2D}(\mathbf{q})=\tfrac{1}{2}\lambda_1(\mathbf{q})|e_1(\mathbf{q})|^2+\tfrac{1}{2}\lambda_2(\mathbf{q})|e_2(\mathbf{q})|^2\ . \tag{4}$$

Comparison of Eqs. (3) and (4) then gives

$$\lambda_1=\tfrac{1}{2}(\alpha+\beta)-\tfrac{1}{2}[(\alpha-\beta)^2+4\gamma^2]^{1/2}\ ,$$
$$\lambda_2=\tfrac{1}{2}(\alpha+\beta)+\tfrac{1}{2}[(\alpha-\beta)^2+4\gamma^2]^{1/2}\ ,$$
$$a=\frac{\alpha-\lambda_1}{[(\alpha-\lambda_1)^2+\gamma^2]^{1/2}}\ ,$$
$$b=\frac{\gamma}{[(\alpha-\lambda_1)^2+\gamma^2]^{1/2}}\ . \tag{5}$$

We next consider the scattered intensity $I(\mathbf{q})\sim\langle|\delta\epsilon_{if}|^2\rangle$, where $\delta\epsilon_{if}=\boldsymbol{\pi}_f\cdot\delta\boldsymbol{\epsilon}\cdot\boldsymbol{\pi}_i$ and $\boldsymbol{\pi}_{i,f}$ are defined above. Allowing for fluctuations in the tilt angle with respect to the z axis, $\omega(\mathbf{q})$, and fluctuations of the in-plane director, $\phi(\mathbf{q})$, we obtain

$$\delta\epsilon_{if}=\epsilon_a\sin\Phi_0(\cos\theta\sin\Phi_0\cos2\chi+\sin\theta\cos\Phi_0\cos\chi)\phi(\mathbf{q}) -\epsilon_a\sin\chi(\cos\theta\sin2\Phi_0\cos\chi+\sin\theta\cos2\Phi_0)\omega(\mathbf{q}) \equiv f_1(\theta,\chi,\Phi_0)\phi(\mathbf{q})-f_2(\theta,\chi,\Phi_0)\omega(\mathbf{q})\ , \tag{6}$$

where $\epsilon_a=\epsilon_\parallel-\epsilon_\perp$ and we have ignored the biaxiality of the Sm-C director. Although we do not allow fluctuations of the tilt with respect to the layer normal, the layer normal still fluctuates with respect to the z axis due to undulations so that

$$\omega(\mathbf{q})=-iu(\mathbf{q})(q_x+q_y\phi)\approx-iq_x u(\mathbf{q})=\frac{q_x}{q_0}\psi(\mathbf{q})\ ,$$

since $\langle\phi\rangle=0$. Rewriting $\delta\epsilon_{if}$ in terms of the normal modes

$$\delta\epsilon_{if}=g_1(\theta,\chi,\Phi_0)e_1(\mathbf{q})+g_2(\theta,\chi,\Phi_0)e_2(\mathbf{q})\ ,$$

where $g_1=af_1-b\tilde{f}_2$, $g_2=bf_1+a\tilde{f}_2$, and $\tilde{f}_2=(q_x/q_0)f_2$, we finally obtain

$$I(\mathbf{q})\sim g_1^2\langle|e_1(\mathbf{q})|^2\rangle+g_2^2\langle|e_2(\mathbf{q})|^2\rangle =g_1^2\frac{k_B T}{\lambda_1(\mathbf{q})}+g_2^2\frac{k_B T}{\lambda_2(\mathbf{q})}\ . \tag{7}$$

In the last step, we have applied the equipartition theorem. With our definition of ψ, we have $\alpha(\mathbf{q})>\beta(\mathbf{q})$, so by choosing the minus sign for λ_1 in Eq. (5), we find for small $\gamma(\mathbf{q})$, $\lambda_1(\mathbf{q})\simeq\beta(\mathbf{q})$. We may then associate $e_1(\mathbf{q})$ with the fast mode and $e_2(\mathbf{q})$ with the slow mode. We note here that $\tilde{f}_2=0$ in the bend and splay geometry; thus we would not expect any scattering from pure undulations at $\chi=0°$ or 90°, in agreement with Fig. 2. This suggests that the coupling terms D_1 and D_2 may be small.

To gauge the significance of the coupling terms, we turn to Fig. 3. In this figure, the dashed lines show a fit assuming negligible surface tension ($\sigma=0$) and no coupling ($D_1=D_2=0$), while the solid lines are fit with coupling. The results in Figs. 3 and 5 are fit simultaneously using the same parameters. The fast-mode data are fit equally well with and without the coupling parameters D_1 and D_2. However, the slow-mode behavior in Fig. 5

is improved by including the coupling. As we pointed out above, the intensity data in Fig. 5 decay more slowly than q^{-2}, especially for the fast mode. This can be explained by the fact that with $\chi=30°$ and $\Phi_0\sim35°$, f_1 increases with q. On the other hand, f_2 has a weak q dependence. This, in combination with the assumed negligible effects of surface tension, explains why the slow-mode intensity decreases only slightly more slowly than q^{-2}. Our model fails to account for the small peak near $\chi=65°$ in the slow-mode χ scan. This peak was observed in all samples we studied. Because the model does not describe the data well for the slow mode in the region where $q_y>q_x$, our fits are insensitive to C_{12}, C_2, and D_2 and thus these parameters are poorly determined. The fit in Figs. 3 and 5 yields values of $C_1l/K_B=3.4(\pm0.3)$, $D_1l/K_B=0.9(\pm0.5)$, $K_S/K_B=4.6(\pm0.4)$, $C_{12}/C_1=5.5(\pm3.1)$, $C_2/C_1=75(\pm24)$, and $D_2/D_1=0.4(\pm0.8)$. For stability, we require K_B, K_S, C_1, C_{12}, and C_2 to be positive. However, the signs of D_1 and D_2 are undetermined. Stability also requires

$$C_{12}^2-C_1C_2<0,\quad C_1K_B-D_1^2l>0,\quad C_2K_S-D_2^2l>0\ .$$

We see that the above values satisfy these constraints.

To obtain the temperature dependence of K_B, K_S, C_1l, and D_1l, we fixed the ratios C_{12}/C_1, C_2/C_1, and D_2/D_1 to the values given above. Also, to obtain reliable results for K_B, it was necessary to fix the tilt angle. We fixed Φ_0 at 32.2° in the Sm-C phase and allowed it to increase to 38.6° in the vicinity of T_{CI}, in reasonable accordance with previous bend and splay mode results [7]. The results of our fits of the fast- and slow-mode intensities to Eq. (7) are shown in Fig. 7. This figure shows the temperature dependence of both the in-plane elasticity K_B and the smectic layer rigidity constant, $\kappa\equiv C_1l$, when $q_y=0$, in the vicinity of the liquid-hexatic transition, $T_{CI}\approx83.6$ °C. Here we plot C_1l scaled to K_B for $T\sim T_{CI}$, and we find

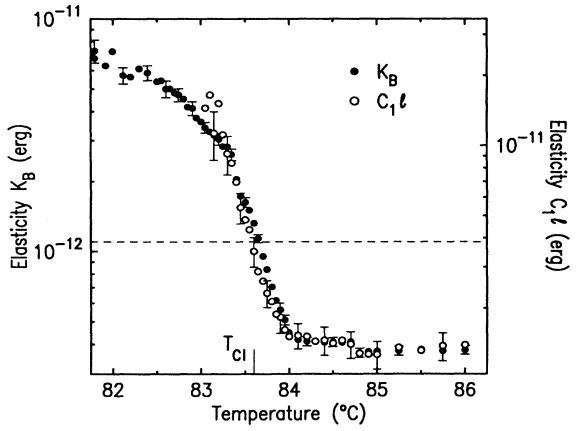

FIG. 7. Temperature dependence of K_B and C_1l are shown. The parameters were determined from fits with Φ_0, C_{12}/C_1, C_2/C_1, and D_2/D_1 fixed, as discussed in the text. The difference in the left (K_B) and right (C_1l) scales indicates $C_1l\approx3.5K_B$. The dashed line indicates the theoretical isotropic hexatic stability limit $72k_BT_{CI}/\pi$ with $T_{CI}=83.6$ °C [12].

$C_1l\approx3.5K_B$ for all T over which C_1 could be reliably extracted. For $T\ll T_{CI}$, we were unable to measure the slow decay on the correlator due to the small intensity and large τ_s. The dashed line in Fig. 7 indicates the isotropic hexatic stability limit. To account for the simple scaling of C_1l and K_B near T_{CI} in the present model of coupled in- and out-of-plane fluctuations, we consider the renormalization of the layer rigidity due to in-layer hexatic ordering. This has been calculated [13] for hexatic-B films of negligible surface tension:

$$\kappa=\tilde{\kappa}-\frac{3k_BT}{4\pi}\ln\frac{L}{\xi}+\frac{3k_BT}{16\pi\tilde{\kappa}}K_A\ln\frac{L}{\xi}\ ,$$

where $\tilde{\kappa}$ is a "bare" rigidity, K_A is the hexatic stiffness constant, L is the sample size, and ξ is the positional correlation length. We can use this to estimate the renormalization of the rigidity in an anisotropic smectic-I film by replacing κ by C_1, K_A by the full elasticity for acoustic bond-tilt fluctuations, $K_B=K_1^B+K_6^I$, and ξ by ξ_1, the in-plane positional correlation length for $q_y=0$, to obtain

$$C_1=\tilde{C}_1-\frac{3k_BT}{4\pi l}\ln\frac{L}{\xi_1}+\frac{3k_BT}{16\pi\tilde{C}_1l^2}K_B\ln\frac{L}{\xi_I}\ . \tag{8}$$

Previous x-ray results indicate that for $T\gg T_{CI}$, $\xi_I\approx10$ Å and $\ln(L/\xi_I)\approx16.1$ ($L\approx1$ cm), while for $T\ll T_{CI}$, we have 200 Å and 13.1, respectively [6]. Thus, the factor $\ln(L/\xi_I)$ in Eq. (8) is essentially constant over the range of T in Fig. 7, and Eq. (8) indicates that the temperature dependence of C_1l should scale simply as K_B, as observed. At high temperature, where $K_6^I\to0$ so that $K_B\approx K_1^B$, the data of Fig. 7 give $C_1l\approx10^{-12}$ erg, in agreement with order-of-magnitude estimates for the rigidity constant of a 2D fluid membrane [14].

Until now we have ignored the effect of the surface tension in our analysis. Since our slow-mode fits are dominated by the functional form of $\tilde{f}_2$ and by C_1l, additional parameters in the free energy coupled to u will have little effect on the scattered intensity. However, we find that our results give $C_ilq_\perp^2\sim(10^{-12}\times10^8)\sim10^{-4}$ dyn/cm. One may take a typical surface tension at a fluid/gas interface to be ~10 dyn/cm. Thus, on first consideration, the surface tension should dominate the terms in u in our free energy, and provide the major restoring force for film undulations. This would give much reduced scattering and an intensity that is independent of q, contrary to our observations. However, in our experiment we are dealing with a thin membrane in contact with a reservoir (the excess material on the sample holder). Under these conditions, the effective surface tension is enormously reduced, as has been discussed theoretically in Ref. [15]. This reference considers a black film with N molecules and a surface area S_0 in contact with a reservoir. By minimizing a Gibb's free energy of the form

$$G=N\phi(\rho)-\mu_rN\ ,$$

where ϕ is the free enthalpy density, $\rho=N/S_0$ is the surface density, and μ_r is the chemical potential of a molecule in the reservoir, one obtains an equilibrium density ρ_0 slightly smaller than the minimum of the free enthalpy

ρ^*, and a surface tension proportional to

$$-\phi'(\rho_0) \simeq \phi''(\rho^*)(\rho^* - \rho_0) ,$$

which is a small number. In fact, this result was obtained for a two-component lyotropic system, where the volume fractions of the components may differ slightly in the film and the reservoir; for a single-component thermotropic system, we might expect the right-hand side to be negligibly small. These considerations provide a plausible explanation for why the surface-tension contribution to the free energy of our film is so much smaller than the elastic curvature energy.

The dynamical behavior of the slow mode, shown in Fig. 6, remains a significant puzzle to us. The dispersion relation for the usual smectic-layer undulation mode would have $\Gamma \sim (C_1 l q_x^2 + C_2 l q_y^2)/\eta_{2D}$, where η_{2D} gives the damping due to the film. This both has a hydrodynamic dependence on q and, for the q's studied, predicts a very large $\Gamma \sim 10^6$ sec^{-1}. The extremely slow and q-independent decay observed suggests a macroscopic motion of the film surface, where the dominant damping could come from the nitrogen gas that surrounds the film. Yet we would not expect such a motion to produce scattering at the experimental $q \sim 10^4$ cm^{-1}, unless, perhaps, it were coupled in some way to more conventional short-wavelength undulations, whose dynamical decay was too fast to detect. Another possible origin for the slow decay would be the diffusion of a yet undescribed textural defect in the director alignment, perhaps characterized by a gradient in the tilt angle itself, which could cause a slight buckling of the film surface at optical q. In this context, we note that the diffusion of vortex defects in the *in-place* director field may be expected to be nonhydrodynamic because of strong coupling to the dynamics of free disclinations in the bond orientations [16]. However, the extremely slow time scale for the diffusion of textural defects, as well as the observed dependence of the intensity on q and χ, would have to be explained.

We were not able to construct a model that leads to a q-independent decay constant (Fig. 6), combined with the q and χ dependence of the intensity (Fig. 5) predicted by Eq. (7), for our experimental range of q. Consequently we do not have a model that satisfactorily explains all of our static and dynamic measurements. Finally, as Fig. 8 shows, Γ_S for the slow mode decreases sharply with temperature in the vicinity of the liquid-hexatic phase transition. Interestingly, this temperature dependence is quite similar to that measured (and also predicted [16]) for

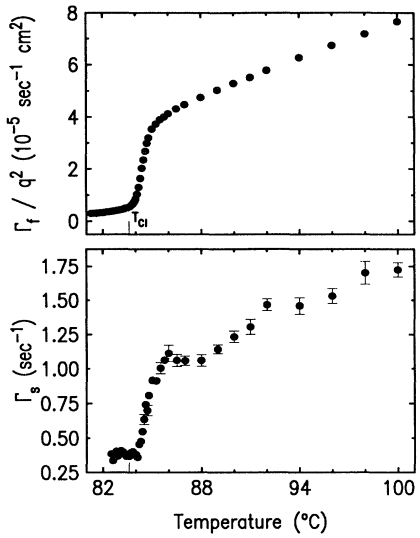

FIG. 8. Temperature dependence of the two observed decay constants are shown. In the top panel, the fast-mode diffusion constant Γ_f/q^2 is shown, while the bottom panel shows Γ_s for the slow mode. These values are derived from the q-scan fits such as the one shown in Fig. 6.

acoustic distortions of the in-plane bond-tilt field (the fast mode). Thus, both the elastic modulus and the decay constant characteristic of the slow mode scale with the analogous quantities for the fast (hydrodynamic) mode at $T \sim T_{CI}$.

In conclusion, our dynamic-light-scattering experiments on a freely suspended film have revealed the presence of a previously unreported slow, nonhydrodynamic mode. The scattered intensity of this mode leads us to associate it with undulations of the film surface, although we find that the linewidth of this mode is independent of q for $q = 8500$–$42\,400$ cm^{-1} in a geometry where it scatters strongly ($\chi = 30°$). Experiments over a greater range of q would be useful, especially for $q_\perp \to 0$, i.e., near specular reflection. In that case, one could rigorously test for the possibility of a nonhydrodynamic component in the intensity; such geometries could not be studied in our present apparatus.

This research was supported by the National Science Foundation under Grant Nos. DMR-8619234 and DMR-9014886 (M.S.S. and J.D.L.), and DMR-8813164 and DMR-911389 (S.S.).

[1] Y. Galerne, J. L. Martinand, G. Durand, and M. Veyssie, Phys. Rev. Lett. **29**, 562 (1972)
[2] Orsay Group on Liquid Crystals, Solid State Commun. **9**, 653 (1971).
[3] C. Y. Young, R. Pindak, N. C. Clark, and R. B. Meyer, Phys. Rev. Lett. **40**, 773 (1978).
[4] S. Sprunt and J. D. Litster, Phys. Rev. Lett. **59**, 2682 (1987).
[5] S. B. Dierker and R. Pindak, Phys. Rev. Lett. **59**, 1002 (1987).
[6] J. D. Brock, D. Y. Noh, B. R. McClain, J. D. Litster, R. J. Birgeneau, A. Aharony, P. M. Horn, and J. C. Liang, Z. Phys. B **74**, 197 (1989).
[7] S. Sprunt, M. S. Spector, and J. D. Litster, Phys. Rev. A **45**, 7355 (1992).
[8] C. W. Garland, J. D. Litster, and K. J. Stine, Mol. Cryst. Liq. Cryst. **170**, 71 (1989).
[9] P. G. de Gennes, *The Physics of Liquid Crystals* (Clarendon, Oxford, 1974).
[10] A. Saupe, Mol. Cryst. Liq. Cryst. **7**, 59 (1969).

[11] D. R. Nelson and B. I. Halperin, Phys. Rev. B **21**, 5312 (1980).
[12] D. R. Nelson and B. I. Halperin, Phys. Rev. B **19**, 2457 (1979).
[13] D. R. Nelson and L. Peliti, J. Phys. (Paris) **48**, 1085 (1987).
[14] W. Helfrich, J. Phys. (Paris) **46**, 1263 (1985).
[15] F. Brochard, P. G. de Gennes, and P. Pfeuty, J. Phys. (Paris) **37**, 73 (1976).
[16] A. Zippelius, B. I. Halperin, and D. R. Nelson, Phys. Rev. B **22**, 2514 (1980).